Journal of Zhejiang University SCIENCE A
ISSN 1673-565X (Print); ISSN 1862-1775 (Online)
www.zju.edu.cn/jzus; www.springerlink.com
E-mail: jzus@zju.edu.cn

# In-vivo retinal imaging by optical coherence tomography using an RSOD-based phase modulator*

Ling WANG[1], Zhi-hua DING[†‡1], Guo-hua SHI[2], Yu-dong ZHANG[2]

([1]*State Key Laboratory of Modern Optical Instrumentation, Zhejiang University, Hangzhou 310027, China*)

([2]*Institute of Optics and Electronics, Chinese Academy of Sciences, Chengdu 610209, China*)

[†]E-mail: zh_ding@zju.edu.cn

Received Feb. 21, 2008; Revision accepted July 2, 2008; Crosschecked Feb. 9, 2009

**Abstract:** Fourier-domain rapid scanning optical delay line (RSOD) was introduced for phase modulation and depth scanning in a time-domain optical coherence tomography (TD-OCT) system. Investigation of parameter optimization of RSOD was conducted. Experiments for RSOD characterization at different parameters of the groove pitch, focal length, galvomirror size, etc. were performed. By implementing the optimized RSOD in our established TD-OCT system with a broadband light source centered at 840 nm with 50 nm bandwidth, in vivo retina imaging of a rabbit was presented, demonstrating the feasibility of high-quality TD-OCT imaging using an RSOD-based phase modulator.

**Key words:** Optical coherence tomography (OCT), Phase modulation, Retina imaging
**doi:**10.1631/jzus.A0820126 **Document code:** A **CLC number:** Q631

## INTRODUCTION

Optical coherence tomography (OCT) functions as a type of optical non-invasive non-contact diagnostic technology, offering in vivo imaging of the human retina with unprecedented sensitivity and axial resolution (Drexler *et al.*, 2001; 2003; Wollstein *et al*., 2005). In terms of speed and sensitivity, Fourier-domain OCT (FD-OCT) is superior to the time-domain OCT (TD-OCT) (Leitgeb *et al*., 2003), and hence there is a tendency for FD-OCT to replace TD-OCT. However, due to complexity in overcoming the inherent shortcomings of FD-OCT, such as mirror image, decreased signal-to-noise ratio (SNR) with depth range (Hausler and Lindner, 1998; Leitgeb *et al*., 2003; Wojtkowski *et al*., 2004; Drexler and Fujimoto, 2008), and no feasible dynamic focusing mechanism, TD-OCT is still a valuable tool in many cases, especially when dynamic focus tracking is required for high lateral resolution.

In order to acquire images with high SNR, phase modulation for heterodyne detection in TD-OCT is usually introduced to generate a sufficiently large carrier frequency in the interference signal so that there are at least two fringes per coherence length scanned. Many methods have been applied to produce such phase modulation. Hoeling *et al*.(2000) utilized a small light-weight mirror driven by a piezo-stack at its resonance frequency. Tearney *et al*.(1996) used a piezo-tube to stretch optical fiber, but uncontrollable static polarization and dynamic birefringence modulation in the fiber are introduced. An electro-optic phase modulator (EOM) (de Boer *et al*., 2001) and an acousto-optical phase modulator (AOM) (Hitzenberger *et al*., 2003) are also implemented to produce phase modulation. However, in addition to large dispersion caused by an EOM or an AOM, the fiber-based modulator is not convenient for obtaining a 840 nm center wavelength suitable for retina imaging (van den Berg and Spekreijse, 1997; Nassif *et al*., 2004;

‡ Corresponding author

* Project supported by the National Natural Science Foundation of China (Nos. 60878057, 60478040 and 30770685), the Hi-Tech Research and Development Program (863) of China (Nos. 2006AA02 Z4E0 and 2008AA02Z422), the Program for New Century Excellent Talents in University of China (No. NCET-04-0528), and the Natural Science Foundation of Zhejiang Province, China (No. Z603003)

Srinivasan *et al*., 2007), while the free-space modulator requires an expensive high-voltage driver. Tearney *et al*.(1997) proposed the use of a Fourier-domain rapid scanning optical delay line (RSOD) for phase modulation as well as depth scanning, but no detailed analyses are given of the design of the RSOD for the range of depth scanning and the carrier frequency required for accurate envelope demodulation. In this paper, investigation of parameter optimization of the RSOD as a phase modulator and a depth scanner is conducted, and experiments for RSOD characterization at different parameters are performed. By implementing the optimized RSOD in our established TD-OCT system, in vivo retina imaging of a rabbit is given, demonstrating the feasibility of high-quality TD-OCT imaging using RSOD as the phase modulator and depth scanner.

## THEORY

As reported previously (Tearney *et al*., 1997; Rollins *et al*., 1998), RSOD has been developed basically for depth scanning and dispersion compensation, and could be a phase modulator if the pivot center of the galvomirror in the RSOD is offset.

RSOD consists of a grating-lens pair in a folded, double-pass Fourier-domain pulse shaping configuration (Fig.1). When RSOD functions as a phase modulator and a depth scanner, the center frequency $f_0$ and bandwidth $\Delta f$ introduced by RSOD is given by (Rollins *et al*., 1998)

$$f_0 = \frac{4x}{\lambda_0}\frac{\partial\gamma(t)}{\partial t}, \tag{1}$$

$$\Delta f = \frac{4\Delta\lambda}{\lambda_0^2}\left(x - \frac{mf\lambda_0}{d}\right)\frac{\partial\gamma(t)}{\partial t}, \tag{2}$$

where $x$ is the pivot offset of the galvomirror relative to the optical axis, $\gamma$ is the scanning angle of the galvomirror, $d$ is the grating period, $m$ is the diffraction order and takes 1 in most situations, $\lambda_0$ is the center wavelength, $\Delta\lambda$ is the bandwidth, and $f$ is the focal length of the lens.

We define the quality factor relative to bandpass filtering in OCT for accurate envelope demodulation as the ratio between center frequency $f_0$ and bandwidth $\Delta f$. By taking account of the usual situation of

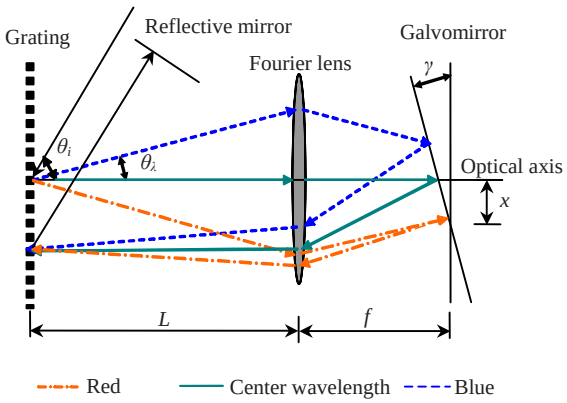


**Fig.1 Schematic of RSOD (view from above)**

$x<<mf\lambda_0/d$, the quality factor is thus determined by

$$\frac{f_0}{\Delta f}/\approx\frac{xd}{f\cdot\Delta\lambda}. \tag{3}$$

For accurate envelop demodulation of the optical heterodyne interferometric signal in OCT, the quality factor should be large enough (Xie *et al*., 2003), and as a rule inequality $f_0/\Delta f\geq 2\sim5$ should be satisfied.

By defining the depth-scanning range as the group delay $l_g$ introduced by RSOD, we have

$$l_g = \frac{4\Delta\lambda}{\lambda_0^2}\left(x - \frac{mf\lambda_0}{d}\right)\gamma. \tag{4}$$

From Eq.(4) we see that a large depth-scanning range can be realized through a highly dispersive grating (Zvyagin *et al*., 2003) or a lens with long focal length (Tearney *et al*., 1997). However, according to Eq.(3), the galvomirror size should be increased proportionally for a bigger offset to provide an adequate carrier frequency required for heterodyne detection. But the increased size of the galvomirror leads to lower oscillation response and hence a lower scanning rate for depth scanning. Therefore, a tradeoff exists between the depth-scanning range and scanning rate; otherwise, the condition for accurate envelop demodulation fails. In addition, a highly dispersive grating requires a lens with a large aperture, posing further optical design challenges. As for a lens with a long focal length and a moderate aperture size, the numerical aperture of the lens decreases and blocks some spectra components of the light source, thus

degrading the depth resolution (Zvyagin *et al*., 2003). When considering Eqs.(3) and (4) simultaneously, we see that a large $\gamma$ can be used for an large depth-scanning range meeting the conditions for accurate envelope demodulation.

## RSOD CHARACTERIZATION

In order to optimize parameters in RSOD for OCT imaging, three sets of parameters for RSOD were investigated by our established TD-OCT system. The system shown in Fig.2 consists of a fiber-based Michelson interferometer illuminated by a broadband light source (SLD-371-HP-DIL-SM-PD, Superlum Diodes Ltd., Russia) with center wavelength $\lambda_0$=840 nm and a full-width-at-half-maximum bandwidth $\Delta\lambda$=50 nm. A flat mirror was used as a sample in the sample arm, and the RSOD under investigation was inserted in the reference arm of the fiber-based Michelson interferometer. The RSOD in the TD-OCT system provides depth scanning and phase modulation.

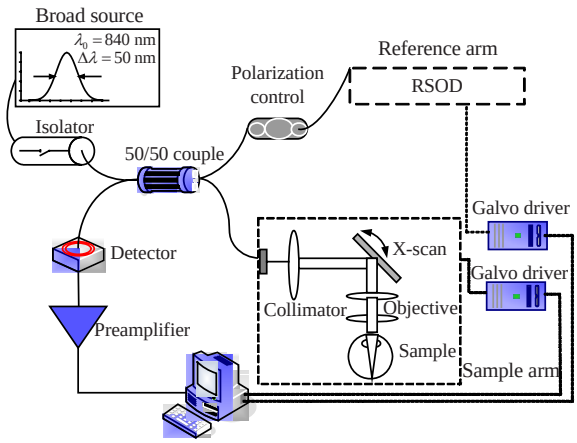


**Fig.2 Schematic of a fiber-based OCT system with RSOD as the phase modulator**

We considered three sets (I, II, and III) of parameters for RSOD as shown in Table 1. We can see that the quality factor $f_0/\Delta f \approx xd/(f\Delta\lambda)$<2 for both sets I and II failed in accurate envelope demodulation. For available grating consideration, we only chose sets II and III for RSOD in the experiments.

First, set II was used for the RSOD. A triangle waveform with a peak-peak value of 0.75 V at 1 kHz was used to drive the galvomirror. The corresponding tilt angle $\gamma$ is 1.5°. From Eqs.(1) and (2) it can be concluded that the center frequency of the interferometric signal is 500 kHz, and the signal bandwidth $\Delta f$=360 kHz. From Eq.(3), it can be seen that the signal envelope could not be completely demodulated, even with a filter with bandwidth wider than the signal bandwidth. For SNR consideration, the digital filter bandwidth was set as $B$=200 kHz. The detected interferometric signal and its envelope demodulated signal are shown in Fig.3. It can be seen that there are less than two fringes per coherence length scanned, and the spectrum of the interference signal becomes aliasing. Artifacts such as ripples and unstable signal amplitude due to incomplete linear demodulation are observed. It should be noted that because the detection bandwidth $B<\Delta f$, it cuts off the signal band and results in a broadening of the demodulated envelope (from 4.52 to 11.92 μs). The demodulated envelope reduces the signal amplitude by about 30% (from 1.04 to 0.73 V).

**Table 1 Three sets of parameters for RSOD**

| Parameter | Value | | |
|---|---|---|---|
| | I | II | III |
| Groove pitch $d$ (mm) | 1/600 | 1/300 | 1/300 |
| Focal length $f$ (mm) | 60 | 60 | 60 |
| Galvomirror size (mm) | 8 | 6 | 8 |
| Feasible offset $x$ (mm) | 3.0 | 2.0 | 3.0 |
| Quality factor $f_0/\Delta f \approx xd/(f\Delta\lambda)$ | <2 | <2 | >2 |

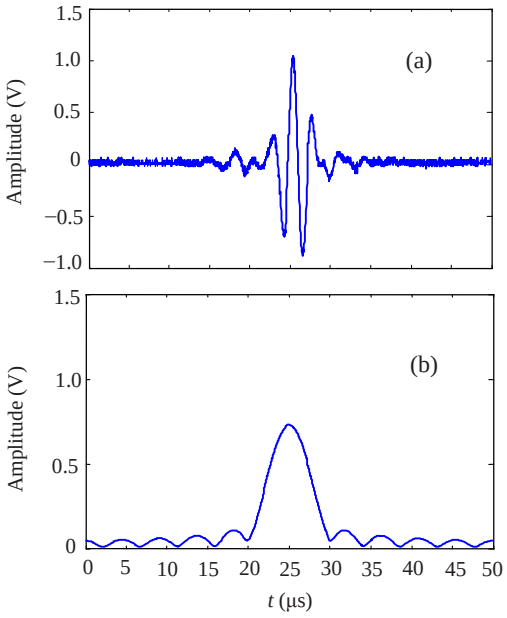


**Fig.3 Detected interferometric signal (a) and its envelope demodulated signal (b) with parameter set II used for RSOD**

Next, set III was used for the RSOD, and a triangle waveform with a peak-peak value of 1.0 V at 500 Hz was used to drive the galvomirror, which permits high A-scan acquisition rates of 500 Hz in the system. The corresponding tilt angle $\gamma$ is 2.0°. From Eqs.(1) and (2), it can be concluded that the center frequency of the interference signal is 500 kHz, and the signal bandwidth $\Delta f$=180 kHz. Because the interference fringes within the low-coherence envelope have increased to 3, accurate demodulation can be easily implemented, as shown in Fig.4. $\Delta T$ is related to the measured coherence length $L_c$=6.8 μm, which is also the depth resolution of the system and close to the theoretical value of 6.23 μm. The depth resolution of our system is higher than that of the current commercially available third generation OCT (OCT 3, 10 μm). The small ripples were caused by the non-Gaussian power spectrum of the light source.

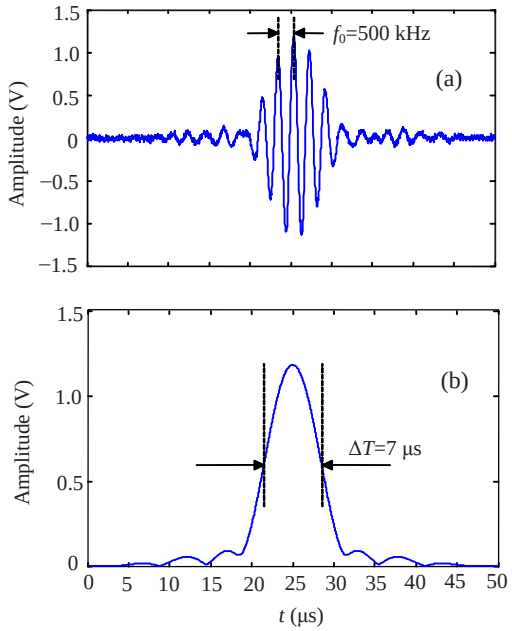


**Fig.4 Detected interferometric signal (a) and its envelope demodulated signal (b) with parameter set III used for RSOD**

Under the condition of accurate envelope demodulation, the amplitude of a driven signal for a galvomirror may be relatively large for an enough depth-scanning range. When a triangular waveform with a peak-peak value of 2.0 V is used to drive the galvomirror, the scanning angle is 4.0° for a depth-scanning range of 3.4 mm, which is enough for retina imaging. To examine the stability of the carrier frequency generated by the RSOD with parameter set III, we measured the carrier frequency of the interference fringes over the whole depth-scanning range. The measured carrier frequency of the interference fringes for optical heterodyne detection varied slightly from 490 to 510 kHz, with the scanning depth (3.4 mm) within a duty cycle of 90%, as shown in Fig.5. The slight fluctuations are mainly due to the nonlinear response of the galvomirror. This relatively stable carrier frequency allows the use of a narrow bandpass filter (ultimately limited by $\Delta f$) to reject off-band noise and thus ensure a high signal-to-noise detection of the OCT signal. The system achieved an SNR of above 100 dB, estimated using calibrated-density filters.

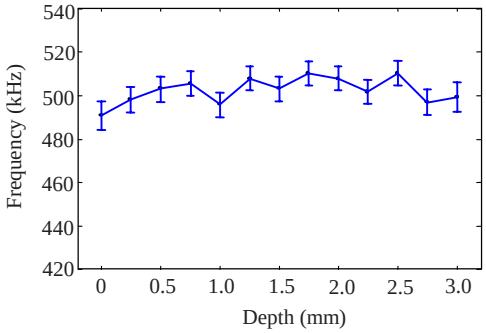


**Fig.5 Measured carrier frequency changes with depth in the OCT scanning system with RSOD at parameter set III**
Frequency variation $\delta f$ is within ±2.5% for a duty cycle of 90%

It can be seen that a relatively low dispersive grating and a relatively large galvomirror permit accurate envelope demodulation and 500 Hz linear depth scanning. The linear depth scanning is quicker than that in the OCT 3 (400 A-scan/s). The amplitude of a driven signal for a galvomirror may be chosen for different depth-scanning range demands in accordance with the prerequisites for accurate envelope demodulation. Therefore, RSOD with parameter set III may be optimal for depth scanning and phase modulation.

## IMAGING APPLICATION

By implementing the RSOD with optimized parameters mentioned above in our established TD-OCT system, in vivo retina imaging of a rabbit was conducted. A rabbit was anesthetized with an intraperitoneal injection of 1.5 g/kg urethane in a 50% solution.

After approximately 20 min the rabbit was sufficiently immobilized. The rabbit was then placed on top of an *XYZ* platform. The right eye of the rabbit was prepared for OCT imaging. Drops of 0.5% (v/v) Alcaine serving as a topical analgesic and 1% (v/v) Atropine to induce mydriasis were administered. A thin, brass eye ring was glued to the equatorial region of the eye with EPIGLU tissue adhesive (Sinomos Ltd., Shanghai, China) and was held in a fixed position to prevent eye motion. A triangle waveform with a peak-peak value of 1.0 V was used to drive the galvomirror, and the corresponding tilt angle $\gamma$ is 2.0°, allowing a depth-scanning range of 1.70 mm according to Eq.(4), which is larger than the thickness of the rabbit's retina. The incident power at the rabbit corner is 500 μW, which is safe for direct beam viewing according to the ANSI laser safety regulations (ANSI, 2000). For detection sensitivity and the estimated frequency of the interferometric signal from Eqs.(1) and (2), the bandwidth of the detector was chosen as 1 MHz.

The measured interferometric signal spectrum is shown in Fig.6, which ensures a high SNR detection of the OCT signal. It can be seen that the system signal center frequency and the bandwidth are $f_0$=500 kHz and $\Delta f$=200 kHz, respectively. The real bandwidth of the interferometric signal is a little larger than the theoretical value, mainly due to the fluctuations of the carrier frequency, but it still ensures the SNR of above 100 dB, estimated using calibrated-density filters. Fig.7 shows in vivo OCT image of the rabbit retina around the fovea center, acquired in 0.25 s. The image consists of 128 A-scans covering about 3 mm in transverse and 1.35 mm in axial direction corresponding to 128 ($x$)×200 ($z$) pixels. The real axial imaging range is less than the theoretical depth-scanning range because of the attenuation of the light and the duty cycle of sampling. The image shows features that can be identified as the nerve fiber layer (NFL), inner plexiform layer (IPL), inner nuclear layer (INL), outer plexiform layer (OPL), external limiting membrane (ELM), outer nuclear layer (ONL), interface between the inner and outer segments of the photoreceptors (OS), and retinal pigment epithelium (RPE). Several blood vessels (indicated with an arrow) and the choroid (Ch) can also be distinguished.

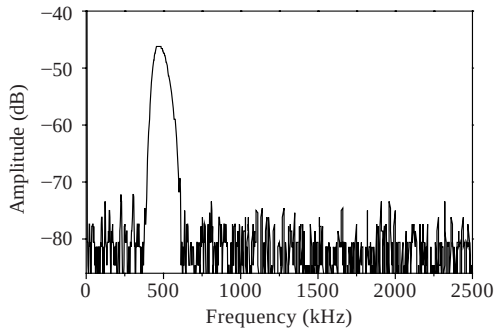


**Fig.6 Frequency spectrum of the interference signal**

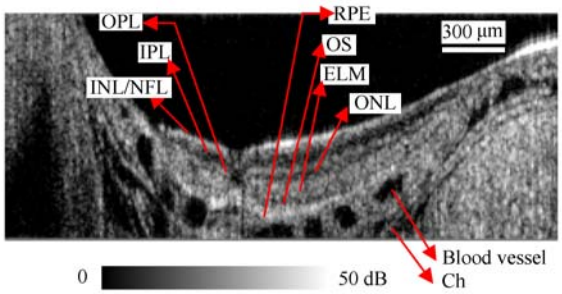


**Fig.7 In vivo OCT image of the rabbit retina around the fovea centers, consisting of 128 depth profiles acquired in 0.25 s**

Dimension is 3.0 mm (width)×1.35 mm (depth). The image shows features that can be identified as the nerve fiber layer (NFL), inner plexiform layer (IPL), inner nuclear layer (INL), outer plexiform layer (OPL), external limiting membrane (ELM), outer nuclear layer (ONL), interface between the inner and outer segments of the photoreceptors (OS), and retinal pigment epithelium (RPE). Several blood vessels (indicated with an arrow) and the choroid (Ch) can also be distinguished

## CONCLUSION

In summary, the optimization of the parameters of the RSOD for depth scanning and phase modulation was conducted, both theoretically and experimentally. It is found that a low dispersive grating and a relatively large size galvomirror used in RSOD permit accurate envelope demodulation and thus enhanced signal-to-noise performance of optical heterodyne detection. The amplitude of the driven signal chosen for the galvomirror may be relatively large to allow an enough depth-scanning range to meet the conditions for accurate envelope demodulation. The variation of the carrier frequency caused by the nonlinear response of the galvomirror is relatively small and acceptable for phase modulation, which has been proved by the

measured SNR of the system. The OCT system centered at 840 nm by implementing the optimized RSOD was established, and in vivo high-resolution rabbit retina imaging results were presented, demonstrating the feasibility of high-quality TD-OCT imaging using an RSOD-based phase modulator.

## References


ANSI, 2000. American National Standards for Safe Use of Lasers. ANSI Z.136.1. American National Standards Institute, USA.

de Boer, J.F., Saxer, C.E., Nelson, J.S., 2001. Stable carrier generation and phase-resolved digital data processing in optical coherence tomography. *Appl. Opt.*, **40**(31):5787-5790. [doi:10.1364/AO.40.005787]

Drexler, W., Fujimoto, J.G., 2008. State-of-the-art retina optical coherence tomography. *Prog. Ret. Eye Res.*, **27**(1):45-88. [doi:10.1016/j.preteyeres.2007.07.005]

Drexler, W., Morgner, U., Ghanta, R.K., Kartner, F.X., Schuman, J.S., Fujimoto, J.G., 2001. Ultra high-resolution ophthalmic optical coherence tomography. *Nat. Med.*, **7**(4):502-507. [doi:10.1038/86589]

Drexler, W., Sattmann, H., Hermann, B., Ko, T.H., Stur, M., Unterhuber, A., Scholda, C., Findl, O., Wirtitsch, M., Fujimoto, J.G., 2003. Enhanced visualization of macular pathology with the use of ultra high-resolution optical coherence tomography. *Arch. Ophthalmol.*, **121**(5):695-706. [doi:10.1001/archopht.121.5.695]

Hausler, G., Lindner, M.W., 1998. Coherence radar and spectral radar—new tools for dermatological diagnosis. *J. Biomed. Opt.*, **3**(1):21-31. [doi:10.1117/1.429899]

Hitzenberger, C.K., Trost, P., Lo, P.W., Zhou, Q.Y., 2003. Three-dimensional imaging of the human retina by high-speed optical coherence tomography. *Opt. Exp.*, **11**(21):2753-2761.

Hoeling, B.M., Fernandez, A.D., Haskell, R.C., Huang, E., Myers, W., Petersen, D., Ungersma, S., Wang, R., Williams, M., Fraser, S., 2000. An optical coherence microscope for 3-dimensional imaging in developmental biology. *Opt. Exp.*, **6**(7):136-146.

Leitgeb, R., Hitzenberger, C.K., Fercher, A.F., 2003. Performance of Fourier domain vs. time domain optical coherence tomography. *Opt. Exp.*, **11**(8):889-894.

Nassif, N.A., Cense, B., Park, B.H., Pierce, M.C., Yun, S.H., Bouma, B.E., Tearney, G.J., Chen, T.C., de Boer, J.F., 2004. In vivo high-resolution video-rate spectral-domain optical coherence tomography of the human retina and optic nerve. *Opt. Exp.*, **12**(3):367-376. [doi:10.1364/OPEX.12.000367]

Rollins, A.M., Kulkarni, M.D., Yazdanfar, S., Ung-arunyawee, R., Izatt, J.A., 1998. In vivo video rate optical coherence tomography. *Opt. Exp.*, **3**(6):219-229.

Srinivasan, V.J., Huber, R., Gorczynska, I., Fujimoto, J.G., Jiang, J.Y., Reisen, P., Cable, A.E., 2007. High-speed, high-resolution optical coherence tomography retinal imaging with a frequency-swept laser at 850 nm. *Opt. Lett.*, **32**(4):361-363. [doi:10.1364/OL.32.000361]

Tearney, G.J., Bouma, B.E., Bopport, S.A., Golubovic, B., Swanson, E.A., Fujimoto, J.G., 1996. Rapid acquisition of in vivo biological images by use of optical coherence tomography. *Opt. Lett.*, **21**(17):1408-1410. [doi:10.1364/OL.21.001408]

Tearney, G.J., Bouma, B.E., Fujimoto, J.G., 1997. High-speed phase- and group-delay scanning with a grating-based phase control delay line. *Opt. Lett.*, **22**(23):1811-1813. [doi:10.1364/OL.22.001811]

van den Berg, T.J., Spekreijse, H., 1997. Near infrared light absorption in the human eye media. *Vis. Res.*, **37**(2):249-253. [doi:10.1016/S0042-6989(96)00120-4]

Wojtkowski, M., Srinivasan, V.J., Ko, T.H., Fujimoto, J.G., Kowalczyk, A., Duker, J.S., 2004. Ultrahigh-resolution, high-speed, Fourier domain optical coherence tomography and methods for dispersion compensation. *Opt. Exp.*, **12**(11):2404-2422. [doi:10.1364/OPEX.12.002404]

Wollstein, G., Paunescu, L.A., Ko, T.H., Fujimoto, J.G., Kowalevicz, A., Hartl, I., Beaton, S., Ishikawa, H., Mattox, C., Singh, O., *et al.*, 2005. Ultra high-resolution optical coherence tomography in glaucoma. *Ophthalmology*, **112**(2):229-237. [doi:10.1016/j.ophtha.2004.08.021]

Xie, T., Wang, Z., Pan, Y., 2003. High-speed optical coherence tomography using fiberoptic acousto-optic phase modulation. *Opt. Exp.*, **11**(24):3210-3219.

Zvyagin, A.V., Smith, E.D., Sampson, D., 2003. Delay and dispersion characteristics of a frequency-domain optical delay line for scanning interferometry. *J. Opt. Soc. Am. A*, **20**(2):333-341. [doi:10.1364/JOSAA.20.000333]